Phase-field simulations and analysis of effect of dispersed particles on migration of delta to gamma transformation interface

Daisuke SATO [a], Munekazu OHNO [b] and Kiyotaka MATSUURA [c]

[a]Graduate Student, Graduate School of Engineering, Hokkaido University, Kita 13 Nishi 8, Kita-ku, Sapporo, Hokkaido, 060-8628 Japan.

[b]Associate Professor, Division of Materials Science and Engineering, Faculty of Engineering, Hokkaido University, Kita 13 Nishi 8, Kita-ku, Sapporo, Hokkaido 060-8628, Japan.

[c]Professor, Division of Materials Science and Engineering, Faculty of Engineering, Hokkaido University, Kita 13 Nishi 8, Kita-ku, Sapporo, Hokkaido 060-8628, Japan.

Abstract

Retardation effect of dispersed inert particles on delta-gamma interface migration in carbon steels during isothermal delta to gamma transformation is analyzed by two-dimensional phase-field simulations. The effect is systematically investigated for different values of particle radius, r, particle spacing, l, and initial carbon concentration of delta phase. The retardation effect becomes stronger when the pinning parameter described by r/l^2 is larger and the carbon concentration of delta phase is higher, indicating that delta to gamma transformation kinetics can be retarded in a similar way to the pinning effect on grain growth kinetics.

I. Introduction

Continuous Casting (CC) process is widely used for the production of steels. In carbon steels with carbon concentration lower than 0.17 mass%, δ to γ transformation occurs during cooling after completion of peritectic reaction [1, 2] or δ solidification, followed by the formation of γ grain structure. Since the temperature for the completion of δ to γ transformation is quite high, γ grains rapidly grow to be coarse [3] and the coarse γ grain structure causes the deterioration in mechanical properties and the occurrence of surface cracking of the CC slabs [3, 4] . Therefore, the grain refinement of γ phase is a very important issue to be tackled in the field of casting of steels.

One of the key parameters in the grain refinement of the γ phase is the temperature for the completion of δ to γ transformation. This temperature is indicated by the thick line in the Fe-C phase diagram shown in **Figure 1**. It is called T_γ in this paper and it corresponds to the temperature for the onset of γ grain growth during cooling. When T_γ is higher, γ grains grow more rapidly. Hence, the reduction of T_γ is effective in retarding the γ grain growth [3] because the mobility of the grain boundary is lower at lower temperatures.

In general, T_γ can be lowered by controlling the cooling rate [5] or by adding alloying elements [5, 6]. For example, T_γ decreases with an increase in the cooling rates, deviating from the equilibrium

value due to the non-equilibrium transformation process. Also, the addition of some alloying elements such as P, Al and Cr reduces the equilibrium value of T_γ [6]. In this study, we focus on a different way of decreasing T_γ, which is based on a retardation effect of dispersed particles on the migration of δ-γ interface. It is well known that the existence of second phase particles in polycrystalline materials retards the migration of grain boundaries, which is called pinning effect [7-10]. The origin of the pinning effect corresponds to the reduction of the total grain boundary energy due to the intersection of the boundary with the particles. One can expect that during the migration of δ-γ interface, the total interfacial energy of δ-γ interface can be reduced when the interface intersects with the particle. The migration of δ-γ interface should accordingly be retarded and the δ to γ transformation should finish at lower temperatures, thus resulting in the reduction of T_γ. Hence, the existence of dispersed particles in δ phase may result in the reduction of T_γ due to the retardation effect similar to the pinning effect in the grain growth. However, care must be paid to the fact that there is a difference between the migration of the grain boundary and that of the δ-γ interface. The former one is the curvature-driven migration, while the latter one is driven by a concentration gap from the equilibrium state and controlled by a solute diffusion process. Therefore, the retardation effect of the particles on the migration of δ-γ interface needs to be investigated in detail for the reduction of T_γ.

In our previous study [11], the effect of ZrO_2 particles on the isothermal peritectic transformation kinetics was investigated by means of a diffusion couple experiment and the existence of retardation effect was confirmed based on the microstructural observations. In addition, the validity of this finding was checked by a phase-field simulation. However, the details of the retardation effect, such as dependencies of the retardation effect on several factors such as particle radius, r, particle spacing, l, alloy composition and the mechanism of the retardation have not been fully elucidated. In particular, it is very important to understand the effects of different values of r and l of the dispersed particle and different initial carbon concentrations in δ phase.

The purpose of this study is to clarify the details of the retardation effect of the particles on the migration of δ-γ interface, such as the dependencies of its magnitude on the particles radius, the particles spacing and the initial carbon concentration. For the investigation, we have employed the phase-field method. Among many simulation methods, this method has been developed as one of the most powerful methods to describe microstructural evolution processes. In this study, we performed two-dimensional phase-field simulations of isothermal δ to γ transformation in Fe-C binary system including inert particles.

II. Phase-field model

A. Multi-phase-field model

In this study, we utilized the multi-phase-field (MPF) model which was originally proposed by

Steinbach et al. [12] to describe microstructural evolution processes in multi-phase systems. The detailed explanation of this model can be found in several articles [12-14]. In this model, a set of phase-fields, $\phi_i(\mathbf{r},t)$, with $i = 1, 2, \cdots, N$ is defined to distinguish N different phases. The phase-field, $\phi_i(\mathbf{r},t)$, is a probability of finding i phase at given position, $\mathbf{r}$, and time, t. In this study, N is equal to 3 and $i = 1$, 2 and 3 corresponds to δ, γ and inert particle (denoted by P) phases. $\phi_i(\mathbf{r},t)$ continuously changes from 1 (inside of i phase) to 0 (outside of i phase) in the interfacial region. The interface has a finite width. The set of ϕ_i should satisfy the following constraint,

$$\sum_{i=1}^{N} \phi_i(\mathbf{r},t) = 1 \quad . \qquad [1]$$

Since our focus is δ to γ transformation, the diffusion of carbon is also calculated. Carbon concentration field, $C(\mathbf{r},t)$, is expressed as a mixture of concentration fields of all coexisting phases, C_i, weighed by ϕ_i as follows,

$$C(\mathbf{r},t) = \sum_{i=1}^{N} \phi_i C_i(\mathbf{r},t) \quad . \qquad [2]$$

The free energy functional of the system is defined as follows,

$$F = \int_V f \mathrm{d}V = \int_V \left(f^{\mathrm{P}} + f^{\mathrm{T}} \right) \mathrm{d}V \quad , \qquad [3]$$

where V is the volume of system and f is the free energy density. It consists of the interfacial potential energy density term, f^{P}, and the thermodynamic potential energy density term, f^{T}, which are respectively defined by

$$f^{\mathrm{P}} = \sum_{j>i}^{N} \sum_{i=1}^{N} \left(-\frac{\varepsilon_{ij}^2}{2} \nabla\phi_i \nabla\phi_j + \omega_{ij} \phi_i \phi_j \right) \quad , \qquad [4]$$

$$f^{\mathrm{T}} = \sum_{i=1}^{N} \phi_i f^i(C_i) \quad . \qquad [5]$$

In Eq. [4] ε_{ij} is the gradient energy coefficient in i-j interface and ω_{ij} is the height of double-well potential between i and j phases. Also, these parameters have the relation, $\varepsilon_{ij} = \varepsilon_{ji}$ and $\omega_{ij} = \omega_{ji}$.
In order to obtain the time evolution equations for $\{\phi_i\}$, we introduce the interface field, ψ_{ij}, as

$$\psi_{ij} = \phi_i - \phi_j \quad . \qquad [6]$$

Then, ϕ_i is rewritten as

$$\phi_i = \frac{1}{n} \left(\sum_{j \neq i}^{N} s_{ij} \psi_{ij} + 1 \right) \quad , \qquad [7]$$

with a step function, s_{ij}, which takes 1 when ϕ_i and ϕ_j coexist and takes 0 otherwise. The total number of the coexisting phases is denoted by n. Utilizing the interface fields, the governing equation of ϕ_i is finally derived as follows,

$$\frac{\partial \phi_i}{\partial t} = -\frac{2}{n}\sum_{j\neq i}^{N} s_{ij} M_{ij}\left(\frac{\delta F}{\delta \phi_i} - \frac{\delta F}{\delta \phi_j}\right) \quad , \qquad [8]$$

where

$$\frac{\delta F}{\delta \phi_i} = \sum_{j\neq i}^{N}\left(\frac{\varepsilon_{ij}^2}{2}\nabla^2\phi_j + \omega_{ij}\phi_j\right) + \left(f^i - \mu_c(C_i)\right) \quad . \qquad [9]$$

The term in the second parentheses of the right-hand side of Eq. [9] is related to the chemical driving force and the derivation of this term was carried out based on the condition of the equal chemical potential for the coexisting phases [15], described as

$$\partial f^i / \partial C_i = \partial f^j / \partial C_j = \cdots = \partial f^N / \partial C_N = \mu_c \quad , \qquad [10]$$

where μ_c is the chemical potential.

Under dilute solution limit, the driving force for the migration of *i*-*j* interface, $f^i - f^j - \mu_c (C_i - C_j)$, can be approximated as [15, 16]

$$f^i - f^j + \mu_c(C_i - C_j) \approx \frac{RT}{V_m}\left(C_{i,e} - C_{j,e} - C_i + C_j\right) \quad , \qquad [11]$$

where V_m is the molar volume of the material, R is gas constant, T is the temperature and $C_{i,e}$ denotes the equilibrium concentration of i phase.

The diffusion equation is given by

$$\frac{\partial C}{\partial t} = \nabla\sum_{i=1}^{N} D_i \phi_i \nabla C_i \quad , \qquad [12]$$

where D_i is the diffusion coefficient of the carbon atom in i phase. In a dilute alloy, the following relation between C_i and C_j is satisfied,

$$k_{ij} = \frac{C_i}{C_j} = \frac{C_{i,e}}{C_{j,e}} = const. \quad , \qquad [13]$$

where k_{ij} is the partition coefficient between i and j phases. In the present simulations, we calculated the carbon diffusion using only C_γ because of Eq. [13].

The governing equations, Eqs. [8] and [12], are calculated numerically based on the second-order central difference method for space and an explicit Euler method for time. In the preliminary simulations, it was found that the numerical solution is stable as long as $dt \leq dx^2/(4M_{\delta\gamma}\varepsilon_{\delta\gamma}^2)$ and $dt \leq dx^2/4D_\delta$ are satisfied. Here, dt and dx are the time step and grid spacing, respectively. We chose dt and dx in such a way that these conditions are satisfied.

B. Phase-field parameters

The equilibrium profile of ϕ_i is given by [13],

$$\phi_i = \frac{1}{2}\left\{1 - \sin\left(-\pi \frac{x}{W}\right)\right\} \quad , \qquad [14]$$

where x is the spatial coordinate and W is the width of the interface which is independent of the type of the interface and was set to $W = 7dx$ in all the simulations. ε_{ij} and ω_{ij} are, respectively, given by

$$\varepsilon_{ij} = \frac{2}{\pi}\sqrt{2W\sigma_{ij}} \quad , \qquad [15]$$

$$\omega_{ij} = \frac{4\sigma_{ij}}{W} \quad , \qquad [16]$$

where σ_{ij} is interfacial energy of the i-j interface. As for M_{ij}, we employed the following expression given in the quantitative model proposed by Ohno et al. [17],

$$M_{ij} = \left(\frac{15}{4}\frac{0.6276 \cdot \varepsilon_{ij}^2}{\omega_{ij} \cdot D_j}\frac{RT_{m,ij}}{V_m}(1-k_{ij})(C_{j,e} - C_{i,e})\Psi_{ij}(\chi_{ij})\right)^{-1} \quad , \qquad [17]$$

$$\Psi_{ij}(\chi_{ij}) = 1 - \frac{1}{2}(1 - k_{ij}D_i / D_j)\chi_{ij} \quad , \qquad [18]$$

where $T_{m,ij}$ is the transition temperature between i and j phases, χ_{ij} is a constant related to the accuracy of the simulation and it was set to zero in this study.

C. Inert particle

In this study, we focused on the δ-γ interface migration into δ phase where particles are dispersed. The particles were regarded as inert particles, viz. the shape, the size and the position of the particles do not change with time and the carbon diffusion into the particles is prohibited. Hence, we assumed $M_{P\delta} = M_{P\gamma} = 0$, $k_{P\delta} = k_{P\gamma} = 0$ and $D_P = 0$. Although the spatial profile of ϕ_P should be given by Eq. [14], we employed the following expression,

$$\phi_P = \frac{1}{2}\{1 - \tanh(-Ax)\}, \qquad [19]$$

with $A = 0.67$. The above expression with this value of A gives a profile of ϕ_p similar to that given by Eq. [14] but we found in preliminary simulations that Eq. [19] is numerically more stable than Eq. [14] in the present conditions.

D. Numerical conditions

We have performed two-dimensional simulations for isothermal δ to γ transformation in a system with the inert particles. **Figure 2** shows the schematic illustration of the system. The grid spacing,

dx, was set to 0.1 μm and the time step, dt, was set to 0.5 μs in all the simulations. It was confirmed that the results were not significantly affected by using a smaller value for dt. The system was held at 1730 K. The initial thickness of γ phase is 10 μm. The particles with the radius, r, and spacing, l, were regularly arrayed in the region of $x \geq 40$ μm. The system size was $l \times 300$ μm^2. Periodic boundary condition was applied along the dotted lines in **Figure 2** and zero-flux boundary condition was applied along the edges of the system (x = 0, 300 μm). The equilibrium concentrations of δ and γ phases, $C_{\gamma,e}$ and $C_{\delta,e}$, at 1730 K are 0.0047 and 0.0024 in mole fraction, respectively, which are obtained from the equilibrium phase diagram of Fe-C system shown in **Figure 1**. The partition coefficient, $k_{\delta\gamma}$, was then set to $k_{\delta\gamma}$ = 0.51. The initial carbon concentration of γ phase was $C_{\gamma,e}$. The initial concentration of particle phase was set to 0. We varied r from 0.375 to 0.624 μm, l from 2.1 to 10 μm. It is noted that a long diffusion layer generally forms in δ phase during δ to γ transformation because of the high diffusivity of carbon in δ phase. In order to diminish the influence of such a long diffusion layer on the results in a finite system size, we focused on the conditions with relatively high supersaturation. The initial carbon concentration of δ phase, $C_{\delta,0}$, was thus varied from 0.0037 to 0.0045 in mole fraction. For simplicity, all the interfacial energies, σ_{ij}, were set to 0.37 J/m^2 which was equal to that of δ-γ interface. The other input parameters are shown in **Table I.**

In order to check the validity of $M_{\delta\gamma}$ given by Eq. [17] and the set of other input parameters, one-dimensional simulations of isothermal peritectic transformation without the particle were carried out and the results were compared with experimental results by Matsuura et al.[21, 22] The simulation results were in good agreement with the experimental results, as is similar to Ref. [17]. It is noted that the multi-phase-field model used in this study is known to generally suffer from anomalous interface effects [16, 19] and therefore our simulations are only qualitatively accurate. Our focus in this study is accordingly directed at the qualitative aspects of the interaction between the moving δ-γ interface and the particle. However, the comparison with the experimental data for the peritectic transformation [21, 22] showed that the accuracy of our simulations with a set of parameters, $M_{\delta\gamma}$, dx and dt is fairly reasonable.

III. Results & Discussion

A. δ-γ interface passing through the particles

First, we focus on the time evolution process of the interface passing through one particle. Initial carbon concentration of δ phase is set to $C_{\delta,0}$ = 0.0045. The snapshots during this process are shown in **Figures 3(a)-(d)**. r is 0.6 μm, l is 6.0 μm in this simulation. Each figure consists of two types of snapshots, the upper and lower of which represent the spatial profiles of the phase-field and the carbon concentration, respectively. In the present simulations, the particle was assumed as the inert particle and hence the size and shape of the particle do not change with time. Although we mentioned that our simulations are only qualitatively accurate in the last section, here it is noted that

the carbon concentration profiles were calculated in the reasonable accuracy in our simulations. In order to check the accuracy, we simulated this process using dx = 0.067 and 0.15 μm in addition to dx = 0.1 μm. The concentration profiles calculated for these different values of dx are not distinguishable. More precisely, the error in the carbon concentration between 0.067 and 0.1 μm is as low as 1.24 %. Hence, it is considered that the concentration shown in Fig. 3 should be accurate enough to discuss the interface between the particle and δ–γ interface.

It is important to note in **Figures 3(a)-(d)** that the planar δ-γ interface is bent when the interface touches the particle and the interface near the particle gets behind that far from the particle in **Figure 3(d)**. The carbon concentration field is also affected by the existence of the particle. The diffusion of carbon is disturbed by the inert particle, toward which the carbon diffusion is prohibited and the carbon concentration field near the particle accordingly differs from that far from the particle. Although this effect is not dominant, this might be significant in the presence of alloying elements with low diffusivity.

To discuss this process in exact detail, we define two positions of δ-γ interface; one is the moved distance of the interface at the edge of y-axis, x_A, and the other is that located at the center of the system, x_B, as indicated in the inset of **Figure 4**. The time change of the gap between them, $\Delta x_{A\text{-}B} = x_A - x_B$, is plotted in **Figure 4**. $\Delta x_{A\text{-}B} = 0$ indicates that the interface is planar. When $\Delta x_{A\text{-}B}$ is positive, x_A is located in front of x_B. The instants indicated by **(a)-(d)** in **Figure 4** correspond to those shown in **Figures 3(a)-(d)**. δ-γ interface is planar shape at the time point **(a)**. Then, the interface gets close to the particle but it does not directly touch the particle at the point **(b)**. However, $\Delta x_{A\text{-}B}$ takes a positive value at the point **(b)** and hence the migration of the interface near the particle is retarded. As understood from **Figure 3(b)**, the carbon diffusion in δ phase is hindered in the vicinity of the inert particle, which causes a delay of the diffusion into γ phase locally and the retardation of migration of δ-γ interface. When the interface touches the particle at the point **(c)**, $\Delta x_{A\text{-}B}$ changes to a negative value, viz. the migration of interface is locally accelerated. The triple junction between δ-γ, γ-P and δ-P interfaces forms in this case and the local shape near the triple junction is determined by the balance between their interfacial energies. According to the interfacial energies employed in this simulation, δ-γ interface at the triple junction forms a right angle with both the δ-P and γ-P interfaces. In order to realize such an energetically-favorable shape, δ-γ interface migration is initially accelerated. However, after this slight acceleration, the migration of interface undergoes the significant retardation (the point **(d)**). As seen from **Figure 3(d)**, this process corresponds to detachment process of δ-γ interface from the particle. The interface passes through the particle in 15-20 ms and recovers the planar shape again at the point **(e)**.

As demonstrated above, the time evolution process of the interface passing through one particle is not a simple but complicated process involving both the acceleration and the retardation. But, it is clear from **Figure 4** that the most sustained process is the retardation process appearing during the

detachment of the interface from the particle. Hence, the migration of interface is retarded on the whole.

B. Effects of particle radius, spacing and initial carbon concentration on migration of δ-γ interface

The results of the interface moving in δ phase with regularly arranged particles are shown in this section. Initial carbon concentration of δ phase was set to $C_{\delta,0}$ = 0.0043. **Figure 5** shows the phase-field profiles in the system with and without (top) the particles. The particle spacing was set to l = 3.1 μm and the particle radius was set to r = 0.375 μm (middle) and 0.625 μm (bottom). The comparison between these three cases clearly indicates that the existence of the particles actually retards the migration of the interface and this effect depends on the size of the particle. The average distance of the interface was calculated during the simulation and its time change is shown in **Figure 6** where the results with no particle and those for r = 0.375, 0.501 and 0.625 μm with l = 3.1 μm are plotted. The larger particle size yields the stronger retardation effect on the migration of the interface. The moved distance of the interface in the system with no particle obeys the parabolic law in which the moved distance, Δx, was proportional to square root of time, t, as follows,

$$\Delta x = a\sqrt{t} \quad , \qquad [20]$$

where a is a parabolic rate constant. Furthermore, the migration of the interface with the particle was well described by Eq. [20]. The parabolic rate constants, a, were obtained for different values of r and l. **Figure 7** shows the dependence of a on r and l. The dotted line indicates the value in the system without the particle and this value is hereafter denoted by a_{noP}. In **Figure 7**, all the values are lower than a_{noP}, which indicates that the retardation effect arises in all the cases focused here. The difference between a and a_{noP} represents the magnitude of the retardation effect. One can see that the retardation effect becomes stronger when r is larger and/or l is smaller. Hence, it is understood that the retardation effect of the particle can be controlled in terms of r and l.

Now, the variation of parabolic rate constant due to the existence of the particles, $\Delta a_{r,l}$ (= $a_{\mathrm{noP}} - a$), is defined. As already mentioned in the introduction, the pinning effect of the grain growth is well-known phenomenon, the theoretical treatment of which was first given by Zener [7]. According to this theory, the pinning effect originates from the decrease in the total area of the moving boundary due to the intersection with the particle. The pinning force, ΔG_{pin}, is given by

$$\Delta G_{\mathrm{pin}} \propto \frac{r}{l^2} \quad , \qquad [21]$$

where r and l are particle radius and particle spacing, respectively. Similarly, it is considered that the retardation of the δ-γ interface is closely related to the decrease in total area of δ-γ interface due to the existence of the particle. **Figure 8** shows the dependence of $\Delta a_{r,l}$ on the parameter of r/l^2. $\Delta a_{r,l}$ increases almost linearly with r/l^2. In other words, it shows that $\Delta a_{r,l}$ increases in proportion to the

pinning force originating from the reduction of the boundary area. Thus, the retardation effect of the particles on the migration of δ-γ interface can be entirely ascribed to the decrease in total interfacial energy due to the intersection of the interface and the particles on the condition of our focus.

Our focus is directed at the effect of the different initial carbon concentration in δ phase, $C_{\delta,0}$, as well. When the carbon diffusion in δ phase with linear concentration gradient is considered, the relation between a_{noP} and $C_{\delta,0}$, according to Hillert [23], is given as

$$a_{\mathrm{noP}} = \frac{C_{\delta,0} - C_{\delta,\mathrm{e}}}{\sqrt{(C_{\gamma,\mathrm{e}} - C_{\delta,\mathrm{e}})(C_{\gamma,\mathrm{e}} - C_{\delta,0})}} \sqrt{D_\delta} \ . \qquad [22]$$

Although this is an approximate form, it is understood that a_{noP} depends on initial carbon concentration, $C_{\delta,0}$. The value of a_{noP} obtained from the simulation is larger when $C_{\delta,0}$ is higher. **Figure 9** shows the dependence of $\Delta a_{r,l}$ on r/l^2 calculated for different initial carbon concentration of δ phase. It can be seen that when $C_{\delta,0}$ is high, the retardation effect becomes relatively remarkable. In any values of $C_{\delta,0}$ within the range of 0.0037-0.0045, the linear relation between $\Delta a_{r,l}$ and r/l^2 was observed when r/l^2 is high. The slope of each curve was obtained for $r/l^2 > 0.02$ μm^{-1} and the result is shown in **Figure 10** where the vertical axis is the slope and the horizontal one is a_{noP} for each $C_{\delta,0}$. It shows that the retardation effect becomes stronger on the interface moving faster (conditions of larger a_{noP}). It can be explained by the fact that the condition with larger a_{noP} causes higher frequency of the interaction between the interface and the particles. Therefore, the retardation is effective on even fast moving δ-γ interface.

According to these results, the retardation effect obtained by the simulations has the following dependence on the simulation conditions.

$$\Delta a_{r,l} \propto \left(\frac{r}{l^2}\right)(a_{\mathrm{noP}}) \ . \qquad [23]$$

It should be noted that this dependence can be held only when the transformation is not completely stopped during the simulation. If a_{noP} is small enough, the pinning force and driving force are balanced and the parabolic relation does not hold.

IV. Conclusions

In this paper, the effect of the inert particles on the migration of δ-γ interface in Fe-C binary system was investigated by means of two-dimensional simulations of multi-phase-field model. We focused on effects of particle radius, r, particle spacing, l, and initial carbon concentration in δ phase, $C_{\delta,0}$. The important findings are summarized as follows.

1) The time evolution process of the interface passing through one particle is not a simple process but a complicated one involving both the acceleration and the retardation. However, the most sustained process is the retardation process appearing during the detachment of the interface from the particle. Hence, the migration of interface is retarded on the whole.

2) The time evolution of the moved distance of δ-γ interface obeys the parabolic law and the effect of the dispersed particle can be well characterized by the parabolic rate constant, a, regardless of the existence of the particles.
3) The retardation effect of the dispersed particles becomes stronger when r is larger and/or l is smaller. Also, the magnitude of the retardation effect increases almost linearly with r/l^2, which indicates that the retardation effect of the dispersed particles on the migration of δ-γ interface is ascribable to the reduction of total area of the moving interface.
4) From the analysis on the effect of different initial carbon concentrations, it was found that the magnitude of the retardation effect is proportional to the parabolic rate constant for the migration of δ-γ interface without the particles. Hence, the retardation is effective on even fast moving δ-γ interface.

It is noted that it is important to study the effect of the other factors such as interfacial energies. δ-γ, γ-P and δ-P interfaces usually possess the different interfacial energies and its balance determines the shape of triple junction, which will significantly affect the magnitude of the retardation effect. There are also important factors such as the shape and the arrangement of the particles. Since these factors can properly be characterized in the three-dimensional system, three-dimensional simulation is indispensable for the highly accurate quantitative evaluation of this retardation effect. In addition, in order to realize the decrease in T_γ during cooling processes, it is necessary to analyze how the retardation effect occurs on non-isothermal condition with finite temperature gradient and cooling rate.

References

1. H. Fredrikson: Met. Sci., 1976, vol. 10, pp. 77-86.

2. H. W. Kerr and W. Kurz: Int. Mater. Rev., 1996, vol. 41, pp. 129-64.

3. Y. Maehara, K. Yasumoto, Y. Sugitani and K. Gunji: Trans. ISIJ, 1985, vol. 25, pp. 1045-52.

4. L. Schmidt and Å. Josefsson: Scand. J. Metall., 1974, vol. 3, pp. 193-99.

5. N. Yoshida, Y. Kobayashi and K. Nagai: Tetsu-to-Hagané, 2004, vol. 90, pp. 198-205.

6. S. Tsuchiya, M. Ohno and K. Matsuura: ISIJ Int., 2010, vol. 50, pp. 1959-64.

7. C. S. Smith: Trans. AIME, 1948, vol. 175, pp. 15-51.

8. R. Elst, J. Humbeeck and L. Delaey: Acta Metall., 1988, vol. 36, pp. 1723-29.

9. P. A. Manohar, M. Ferry and T. Chandra: ISIJ Int., 1998, vol. 38, pp. 913-24.

10. M. Ohno, C. Murakami, K. Matsuura and K. Isobe: ISIJ Int., 2012, vol. 52, pp. 1832-40.

11. L. Chen, K. Matsuura, D. Sato and M. Ohno: ISIJ Int., 2012, vol. 52, pp. 434-40.

12. I. Steinbach and F. Pezzola: Physica D, 1999, vol. 134, pp. 385-93.

13. S. G. Kim, D. I. Kim, W. T. Kim and Y. B. Park: Phys. Rev. E, 2006, vol. 74, pp. 061605-1-061605-14.

14. Y. Suwa, Y. Saito and H. Onodera: Acta Mater., 2007, vol. 55, pp. 6881-94.

15. S.G. Kim, W. T. Kim and T. Suzuki: Phys. Rev. E, 1999, vol. 60, pp. 7186-97.

16. M. Ohno and K. Matsuura: Phys. Rev. E, 2009, vol. 79, pp. 031603-1-031603-15.

17. M. Ohno and K. Matsuura: Acta Mater., 2010, vol. 58, pp. 6134-41.

18. H. Yin, T. Emi, H. Shibata: Acta Mater., 1999, vol. 47, pp. 1523-35.

19. M. Ohno and K. Matsuura: Acta Mater., 2010, vol. 58, pp. 5749-58.

20. P. Gustafson: Scand. J. Metall., 1985, vol. 14, pp. 259-67.

21. K. Matsuura, Y. Itoh and T. Narita: ISIJ Int., 1993, vol. 33, pp. 583-87.

22. K. Mastuura, H. Maruyama, Y. Itoh, M. Kudoh and K. Ishii: ISIJ Int., 1995, vol. 35, pp. 183-87.

23. C. Zener: J. Appl. Phys., 1949, vol. 20, pp. 950-53.

[Figures]

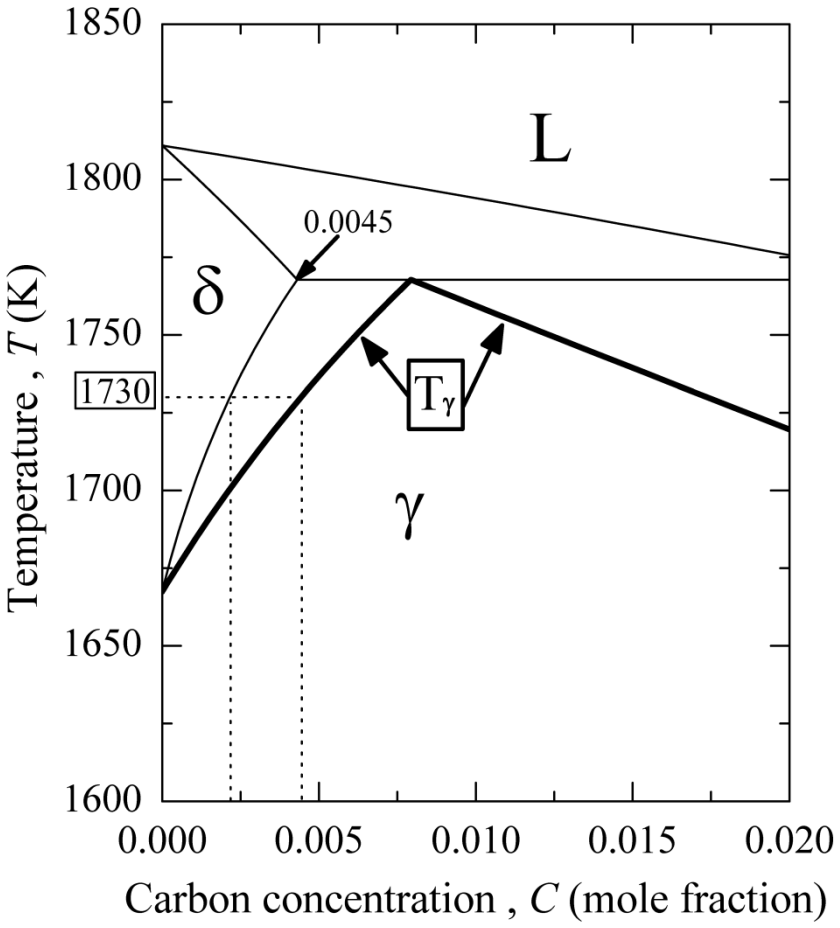

Fig. 1—Calculated phase diagram of Fe-C binary system. The thick line indicates the temperature for the completion of δ to γ transformation, T_γ. The simulations were performed at 1730 K in this study.

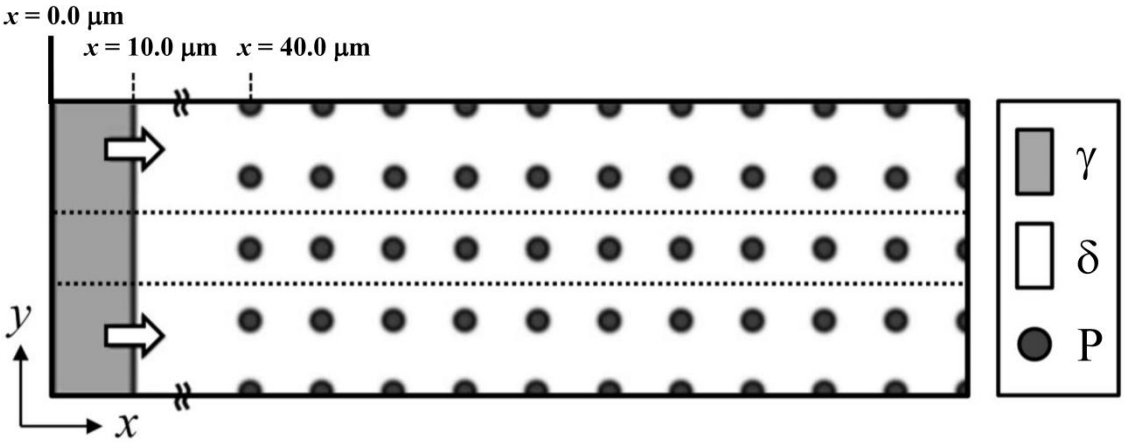

Fig. 2—Schematic illustration of the two-dimensional system we investigated. Periodic boundary condition was applied to *y*-direction along the dotted line and zero-flux boundary condition was applied to *x*-direction. The initial position of δ-γ interface was $x = 10$ μm. The particles, denoted by P, were arranged from 30.0 μm away from the initial position of δ-γ interface.

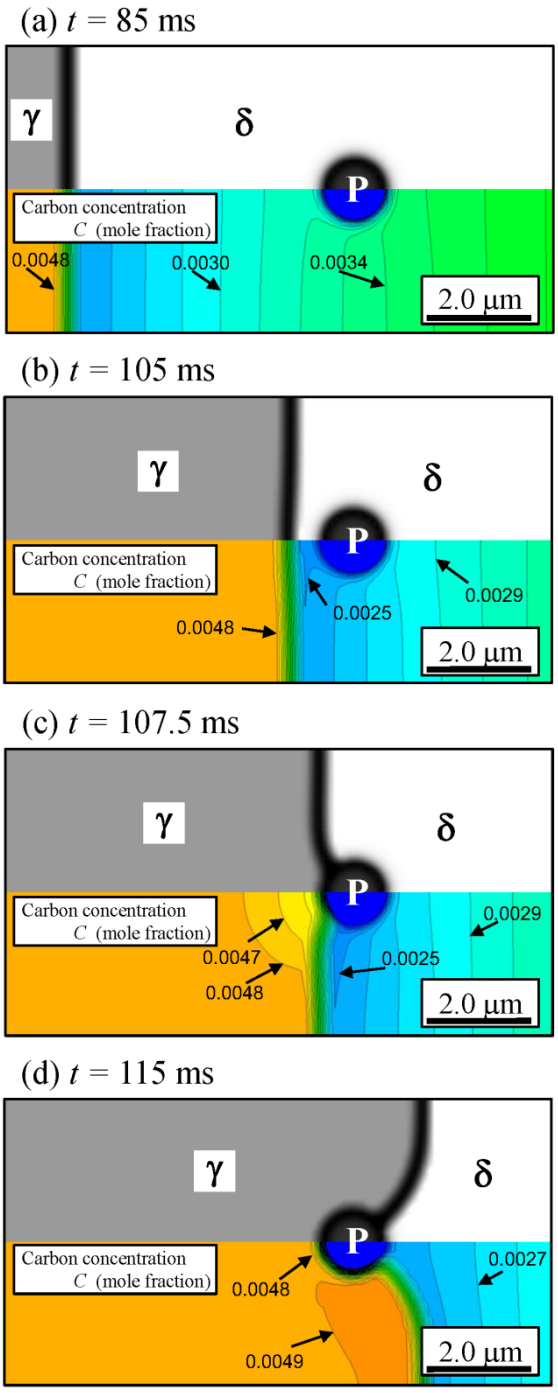

Fig. 3—Time changes of the phase-field and carbon concentration profiles around one particle. Particle radius, r, is 0.6 μm and the length of y-direction, l, is 6.0 μm. Initial carbon concentration of δ phase, $C_{\delta,0}$, is 0.0045 (mole fraction). After step (d) the interface returned to planar shape as in step (a).

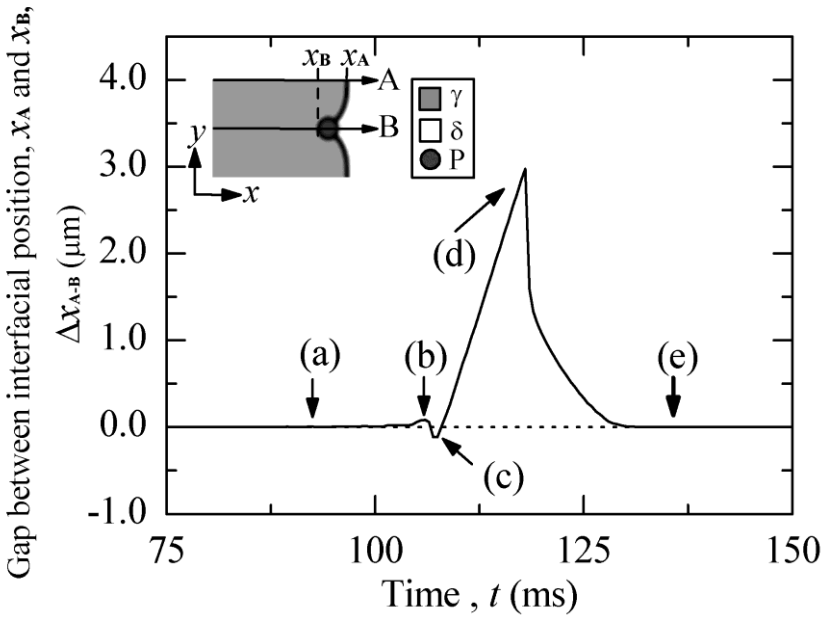

Fig. 4—Time change of the gap between the positions x_A (on the line A) and x_B (on the line B) of δ-γ interface moving in x-direction, $\Delta x_{A\text{-}B} = x_A - x_B$. r is 0.6 μm and l is 6.0 μm. Initial carbon concentration of δ phase, $C_{\delta,0}$, is 0.0045 (mole fraction). The time points indicated by (a)-(d) corresponds to (a)-(d) in Figure 3.

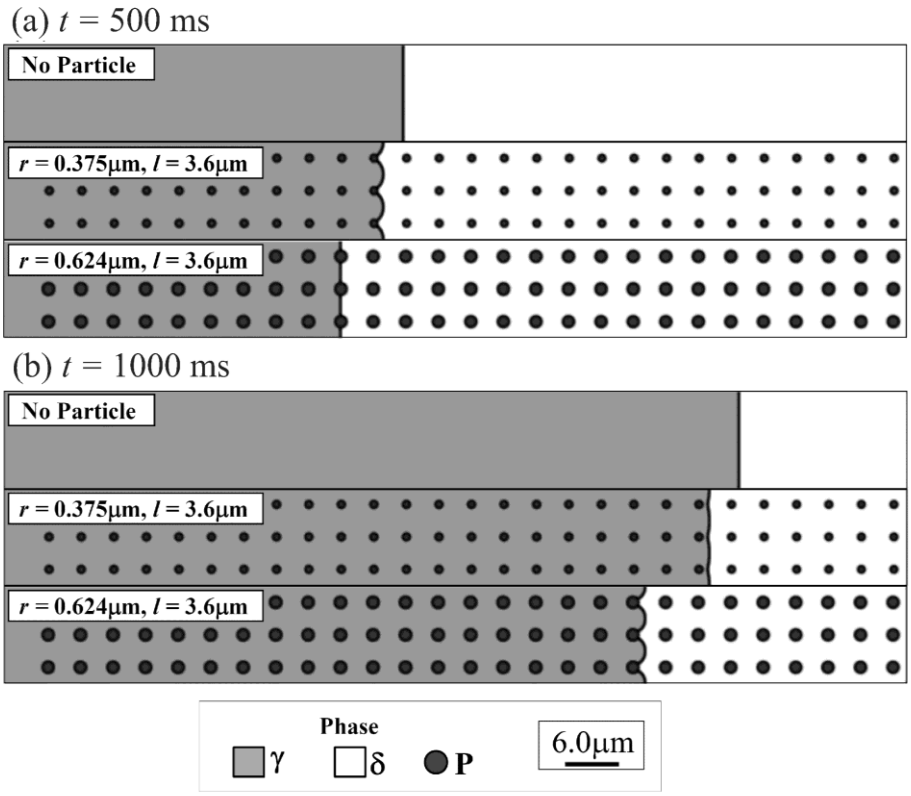

Fig. 5—Phase-field profiles at (a) t = 500 ms and (b) t = 1000 ms calculated without particles (top), r = 0.375 μm, l = 3.6 μm (middle) and r = 0.624 μm, l = 3.6 μm (bottom). $C_{\delta,0}$ is 0.0043 (mole fraction).

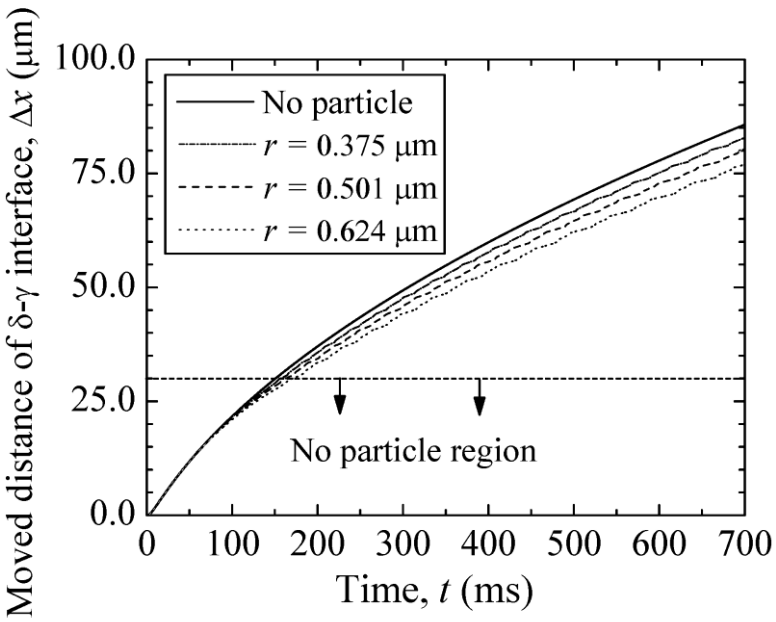

Fig. 6—Time change of the average moved distance of δ-γ interface, Δ*x*, on the particle condition of r = 0.375, 0.501 and 1.000 μm with l = 3.1 μm. $C_{\delta,0}$ is 0.0043 (mole fraction). Solid line indicates the result of No particle condition.

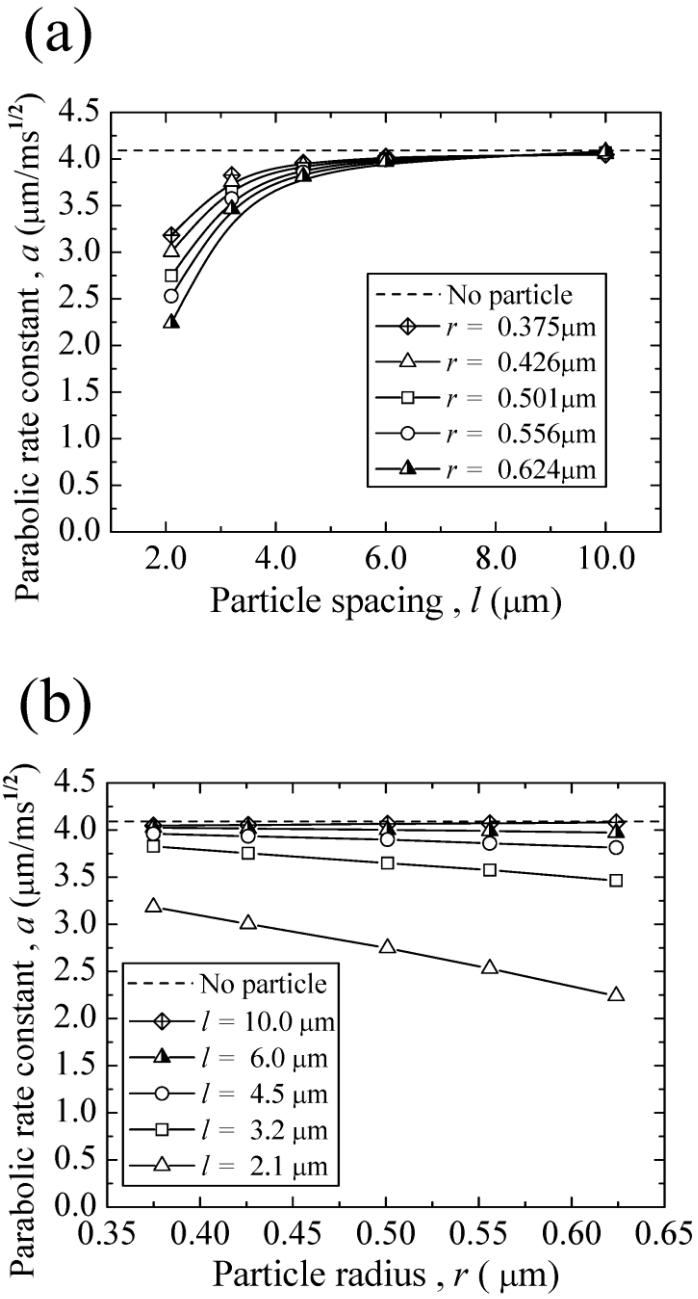

Fig. 7—(a) Dependence of the parabolic rate constant on the particle spacing for various particle radius, *r*. (b) Dependence of the parabolic rate constant on the particle radius for various particle spacing, *l*. $C_{\delta,0}$ is 0.0043. Dotted line is the value obtained without the particle.

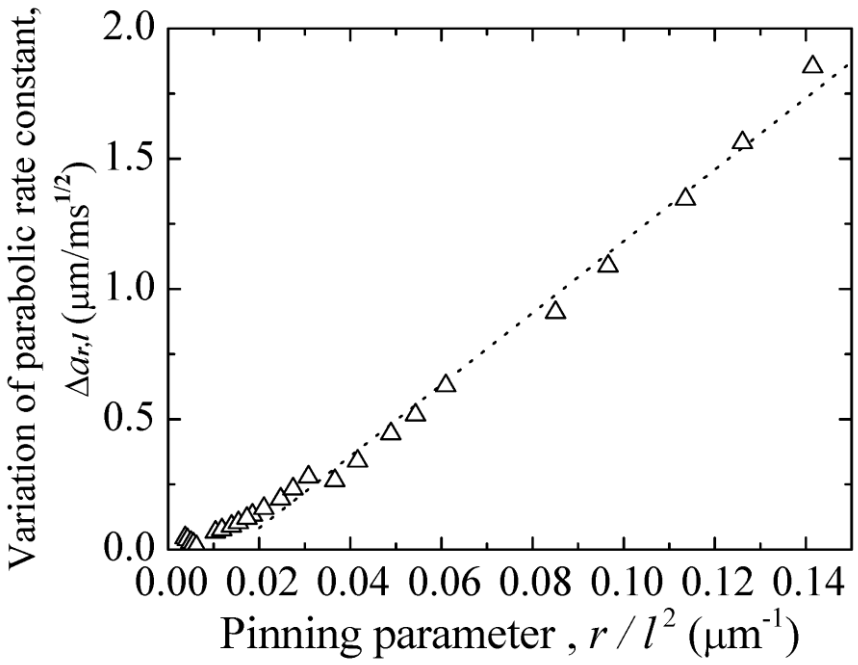

Fig. 8—Zener pinning force ($\propto r/l^2$) dependence of the variation of parabolic rate constant defined as $\Delta a_{r,l} = a_{\mathrm{noP}} - a$. $C_{\delta,0}$ is 0.0043.

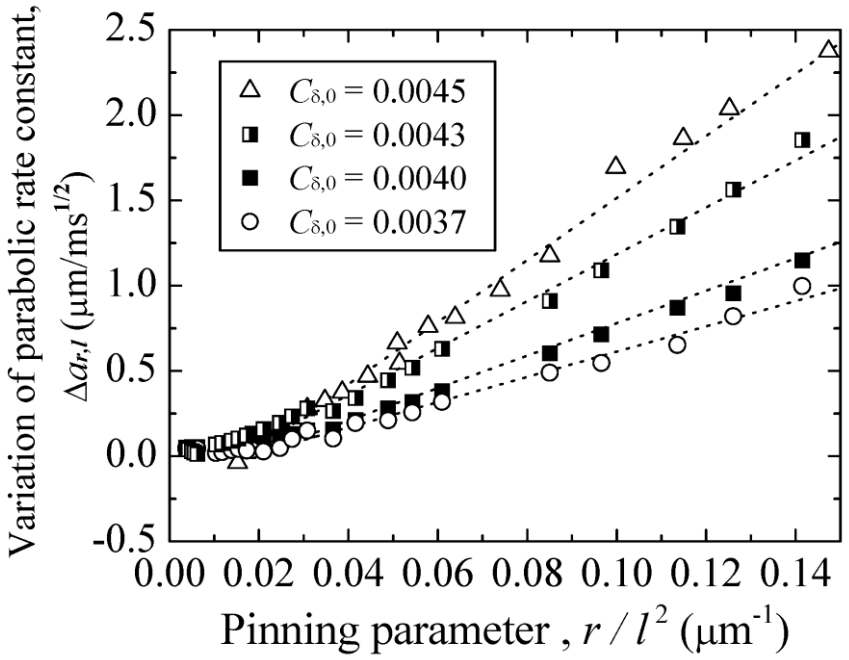

Fig. 9—Dependence of the variation of parabolic rate constant defined as $\Delta a_{r,l} = a_{\mathrm{noP}} - a$ on r/l^2 with various $C_{\delta,0}$ (0.0037-0.0045). Linear relationship exists regardless of $C_{\delta,0}$ when r/l^2 is high.

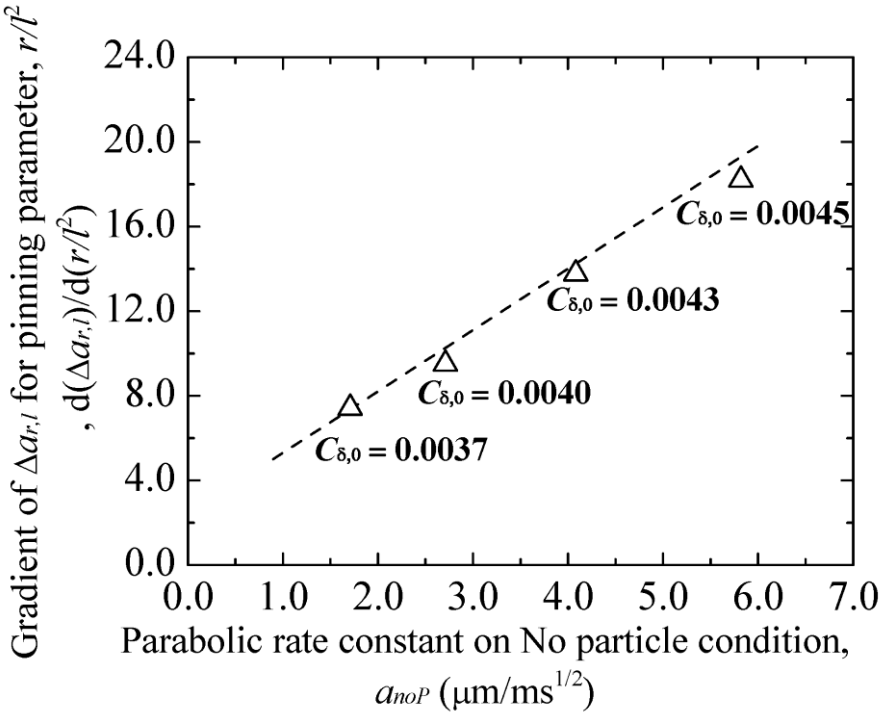

Fig. 10—a_{noP} dependence of the gradient of $\Delta a_{r,l}$ (= $a_{noP} - a$) for pinning parameter, r/l^2, calculated from Figure 9. a_{noP} is related to $C_{\delta,0}$ and driving force of the transformation. Larger a_{noP} condition caused faster migration of the interface and higher frequency of the interaction with the particles, which led to stronger retardation effect on the migration of the interface.